

PCCP

Accepted Manuscript



This is an *Accepted Manuscript*, which has been through the Royal Society of Chemistry peer review process and has been accepted for publication.

Accepted Manuscripts are published online shortly after acceptance, before technical editing, formatting and proof reading. Using this free service, authors can make their results available to the community, in citable form, before we publish the edited article. We will replace this *Accepted Manuscript* with the edited and formatted *Advance Article* as soon as it is available.

You can find more information about *Accepted Manuscripts* in the [Information for Authors](#).

Please note that technical editing may introduce minor changes to the text and/or graphics, which may alter content. The journal's standard [Terms & Conditions](#) and the [Ethical guidelines](#) still apply. In no event shall the Royal Society of Chemistry be held responsible for any errors or omissions in this *Accepted Manuscript* or any consequences arising from the use of any information it contains.



Journal Name

ARTICLE

Improved Performances of PCDTBT:PC₇₁BM BHJ Solar Cells Through Incorporating Small Molecule Donor

Youqin Zhu, ^{†a b} Lin Yang, ^{†c} Suling Zhao, ^{*a b} Yan Huang, ^{*c} Zheng Xu, ^{a b} Qianqian Yang, ^{a b} Peng Wang, ^{a b} Yang Li, ^{a b} and Xurong Xu ^{a b}

Received 00th January 20xx,
Accepted 00th January 20xx

DOI: 10.1039/x0xx00000x

www.rsc.org/

We demonstrate a bulk heterojunction (BHJ) organic photovoltaics (OPVs) with the power conversion efficiency (PCE) of 6.39% by incorporating a small molecular material 2-[4-(N-butyl-N-phenylamino)-2,6-dihydroxyphenyl]-4-[[4-(N-butyl-N-phenylamino)-2,6-dihydroxyphenyl]-2,5-dien-1-ylidene]-3-oxocyclobut-1-en-1-olate (SQ-BP) as the additional donor material into Poly [[9-(1-octylnonyl)-9H-carbazole-2, 7-diyl]-2, 5-thiophenediyl-2, 1, 3-benzothiadiazole-4, 7-diyl-2, 5-thiophenediyl] (PCDTBT) : [6,6]-phenyl C₇₁ butyric acid methyl ester (PC₇₁BM) host binary blend. Incorporating SQ-BP into PCDTBT:PC₇₁BM host blend film increases the photon harvesting of ternary photovoltaic device with a broad absorption spectrum from 300nm to 750nm, which results in an increased short-circuit current density (J_{sc}). In addition to the efficient photon harvesting, Förster resonance energy transfer (FRET) between PCDTBT and SQ-BP is also the reason of the increase of J_{sc}. As a result, the PCE of ternary devices with 10wt% SQ-BP is about 30% greater than that of PCDTBT:PC₇₁BM based binary OPVs.

Introduction

Organic Photovoltaics (OPV) is a candidate of renewable energy technology for its advantages of lightweight, large area, flexible and low-cost, which make it amenable to roll-to-roll high volume production.¹⁻⁴ Many kinds of method have been used to improve the performance of OPVs, such as synthesizing new p-type low-bandgap materials⁵⁻⁸, using effective interlayers⁹⁻¹¹, optimizing device morphology¹²⁻¹⁴ and inventing new device structures^{15, 16}. Recently, the power conversion efficiency (PCE) of organic solar cells has reached 11%¹⁷ for triple-junction polymer solar cell, and 9-10%^{18, 19} for binary polymer:fullerene single-junction solar cells. But there still many factors restrict the performance of OPV, such as limited light harvesting and low carrier mobility, which make the overall PCE of organic solar cells is limited to 10-12%²⁰.

To expand the absorption spectrum of OPV, many kinds of strategy have been studied. Synthesizing new low-bandgap materials is a method, but it takes too much time. The tandem architecture also can broaden the absorption spectrum of OPVs²¹⁻²³ of which the cells allow collecting photons resonant to the bandgap of all used polymer to minimize the thermal losses. However, they are based on a

complicated multi-layer stack with serious technical challenges, such as the processing of a robust intermediated layer, the coupling of light absorption complementary between sub-cells as well as the thickness of solution processed organic active layers in each sub-cell.^{24, 25} Recently, an elegant alternative strategy has been realized to extend the spectral sensitivity of wide bandgap polymers into the near infrared (NIR) region by adding a narrow bandgap sensitizer²⁵⁻³⁰ to form the ternary film which contains two donors and an acceptor or a donor and two acceptors. According to recent research, there are some mechanisms lead to the improvement observed in many ternary solar cells: increased light absorption³¹, improved charge transfer^{32, 33}, energy transfer³⁴, and phase separation³⁵. The improvement of the mechanism above could eventually result in a high-efficiency single-junction organic photovoltaic which can break the proposed efficiency limit of 17%.³⁶

In this article, we demonstrate, for the first time, an efficient bulk heterojunction (BHJ) OPV with PCE of 6.39% by incorporating a small molecular material 2-[4-(N-butyl-N-phenylamino)-2,6-dihydroxyphenyl]-4-[[4-(N-butyl-N-phenylamino)-2,6-dihydroxyphenyl]-2,5-dien-1-ylidene]-3-oxocyclobut-1-en-1-olate (SQ-BP) as the additional donor material into Poly [[9-(1-octylnonyl)-9H-carbazole-2, 7-diyl]-2, 5-thiophenediyl-2, 1, 3-benzothiadiazole-4, 7-diyl-2, 5-thiophenediyl] (PCDTBT) : [6,6]-phenyl C₇₁ butyric acid methyl ester (PC₇₁BM) host binary blend. The BHJ OPV with SQ-BP as the donor and PC₇₁BM as the acceptor showed a PCE of 4.86%, which indicated that SQ-BP is an efficient donor material.³⁷ The PCDTBT absorption shows a spectrum from 350nm to 650 nm and SQ-BP has a near-infrared absorption spectrum from 550nm to 750nm. Incorporating SQ-BP into PCDTBT:PC₇₁BM host blend increases the photon harvesting of photovoltaic device with a broad absorption spectrum from 300nm to 750nm. The photoluminescence (PL) spectrum of PCDTBT has a large range overlap with the absorption

a Key Laboratory of Luminescence and Optical Information (Ministry of Education), Institute of Optoelectronics Technology, Beijing Jiaotong University, Beijing 100044, P. R. China. Corresponding E-mail: slzhao@bjtu.edu.cn

b Institute of Optoelectronics Technology, Beijing Jiaotong University, Beijing 100044, P. R. China.

c Key Laboratory of Green Chemistry and Technology (Ministry of Education), College of Chemistry, Sichuan University, Chengdu 610064, P. R. China. Corresponding E-mail: huangyan@scu.edu.cn

[†] The first two authors contributed equally to this work.

spectrum of SQ-BP shown as Fig. 1(d), which make it possible for Förster resonance energy transfer (FRET) occurred between PCDTBT and SQ-BP. It leads to reduce the energy loss through excitation recombination and enhance the performance of prepared cells.

Experimental

The SQ-BP dye used in this work was synthesized according to the literature procedure.³⁷ PCDTBT (bought from 1 Material Inc) and PC₇₁BM (bought from nano-c) were commercially purchased and used as received. The blend solution of PCDTBT:PC₇₁BM:SQ-BP was prepared as follows: PCDTBT and PC₇₁BM were dissolved in chlorobenzene (CB) with weight ratios of 1:2 with total concentration of 30 mg/mL, and the solution was stirred under a N₂-filling glove box at 30 °C for 12 h. SQ-BP (weight ratios of SQ-BP to PCDTBT were 3, 6, and 10 wt%) were subsequently added to the blend solution. Patterned indium tin oxide (ITO)-coated glass substrates with a sheet resistance of 15 ohm/square were cleaned consecutively in ultrasonic bath containing detergent, acetone, ethanol, and deionized water for 20 min each, and finally blow-dried by high purity nitrogen. The substrates were treated by UV-ozone for 5 min, and 80 Å MoO₃ layer was thermally evaporated onto ITO substrates under a vacuum of 3×10^{-4} Pa at a rate of 0.5 Å/s. The active layers, PCDTBT:PC₇₁BM as a reference and PCDTBT:PC₇₁BM:SQ-BP (1:2:x), were spin-coated onto the MoO₃ films at 2500 rpm for 40 s in a N₂-

filled glovebox. The wet films were slowly and completely dried in covered glass Petri dishes in a N₂-filled glovebox. Finally LiF (7 Å) and Al (1000 Å) films were deposited on the top in a vacuum under a pressure of 3×10^{-4} Pa at a rate of 0.2 Å/s and 1.5 Å/s respectively. The deposition rate and film thickness were in situ monitored by a quartz crystal oscillator mounted to the substrate holder. The active area is 6 mm². The final device structure is ITO/MoO₃/PCDTBT:PCBM:SQ-BP/LiF/Al. The current–voltage curves were measured by using an Abet solar simulator with a Keithley 4200 source measurement unit under AM 1.5 G illumination (100 mW/cm²), after spectral mismatch correction under an ambient atmosphere. The absorption spectrum was measured by Shimadzu UV-3101 PC spectrometer under an ambient atmosphere. The external quantum efficiency (EQE) of the devices were measured by a QE/IPCE Measurements Solar Cell Scan 100 (ZOLIX) system under an ambient atmosphere. Photoluminescence (PL) spectra of films were measured by a Perkin Elmer LS-55 spectrophotometer. The photoluminescence decay were measured by JY TempPro-01-NL under the excitation 373 nm NanoLED. The chemical structures of the organic materials used in this paper is shown in Fig. 1(a) and the device structure of OPVs is shown in Fig. 1(b). The energy level diagrams of different materials used in the device fabrication and carrier transport paths are shown in Fig. 1(c). The PL spectrum of

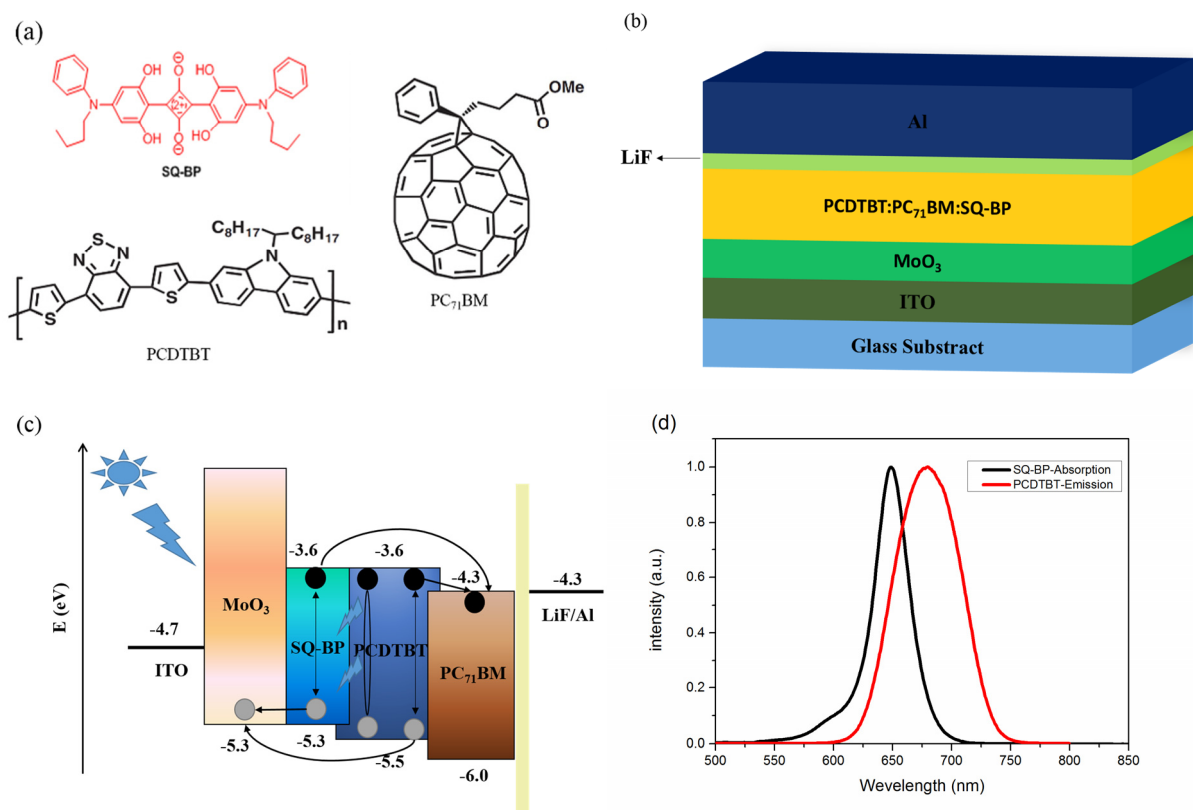


Fig. 1 Material properties and device structure. (a) Chemical structures of SQ-BP, PCDTBT and PC₇₁BM used in here. (b) Device structure of OPVs fabricated in the experiment. (c) The energy level diagrams of different materials used in the device fabrication and carrier transport paths. (d) Photoluminescence (PL) spectra of PCDTBT in chlorobenzene (CB) solution when excited at 450 nm and absorption spectra of SQ-BP in CB solution.

Table 1. Summary of the photovoltaic parameters and efficiencies of solar cells with different ratios of PCDTBT:PC₇₁BM:SQ-BP, measured under AM1.5G Solar Illumination (100 mW/cm²). Rsh and Rs extracted from illuminated J-V curves.

PCDTBT:PCBM:SQ-BP	PCE(%)	Jsc(mA/cm ²)	Voc (V)	FF(%)	PCE ^a (%)	Rsh	Rs
						(Ω cm ²)	(Ω cm ²)
1:2:0	4.91	10.13	0.87	55.77	5.11	535.27	16.76
1:2:0.03	5.46	11.09	0.88	55.97	5.57	633.77	14.49
1:2:0.06	5.83	12.02	0.89	54.54	5.71	426.94	14.27
1:2:0.1	6.39	12.83	0.89	55.91	6.05	439.36	11.57
1:2:0.15	5.68	11.77	0.89	54.29	5.64	373.34	13.82

PCE^a is the average PCE from 16 cell samples.

PCDTBT solution and absorption spectrum of SQ-BP solution are shown in Fig. 1(d).

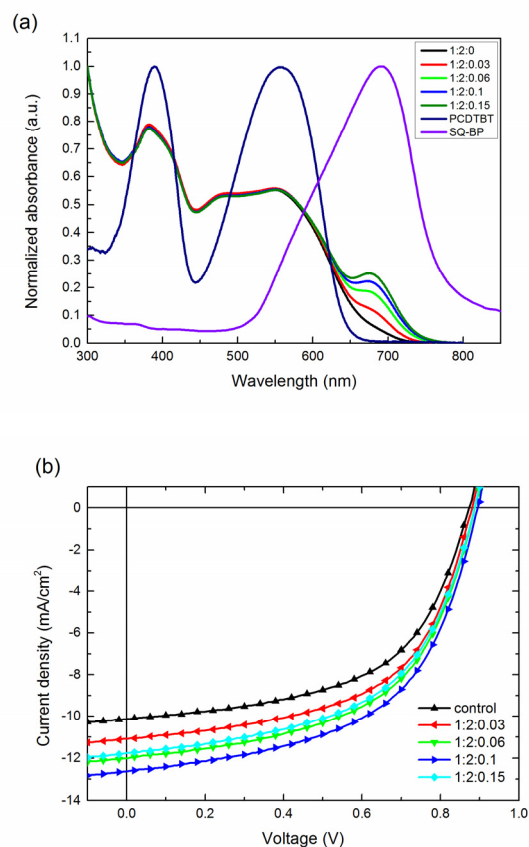
Results and discussion

The ultraviolet–visible (UV–Vis) absorption spectrums of the PCDTBT neat film, SQ-BP neat film and PCDTBT:PC₇₁BM:SQ-BP (1:2:x) ternary blend films are shown in Fig. 2(a). The PCDTBT absorption shows a broad spectrum from 350nm to 650 nm with two peaks at 392 nm and 555nm. The SQ-BP dye has a high extinction coefficient at 647 nm. The absorption intensity from 300nm to 600nm of the blend films don't change with the concentration of SQ-BP. It indicates that the addition of SQ-BP didn't hamper the absorption of PCDTBT and PC₇₁BM. The absorption of the blend films between 650 nm and 750 nm monotonically increased with SQ-BP concentration increased. As a result, the cooperative absorption of PCDTBT and SQ-BP covers a significant part of the solar spectrum, with only limited overlap.

Fig. 2(b) shows the current density – voltage (J–V) characteristics of PCDTBT:PC₇₁BM:SQ-BP devices with different SQ-BP concentrations in the active layer under AM 1.5 G illumination with an intensity of 100 mW/cm². The detail parameters of OPVs are shown in table 1. As we predict that the Jsc of the devices increased with the additive of SQ-BP. The Jsc increased from 10.13 mA/cm² for the control device with PCDTBT:PC₇₁BM as the active layer to 12.83 mA/cm² after added 10 wt% SQ-BP due to the expanded UV–Vis absorption spectral range of the PCDTBT:PC₇₁BM:SQ-BP ternary layer. And the Jsc of the ternary devices monotonously increased by increasing the concentration of SQ-BP, 11.09 mA/cm² for 3wt%, 12.02 mA/cm² for 6wt% and 12.83 mA/cm² for 10wt% respectively. The PCE increased from 4.91% of the control device to 6.39% when the concentration of SQ-BP up to 10wt% coinciding with the tendency of Jsc. But, further adding SQ-BP to 15wt% led to lower Jsc, which was only 11.77 mA/cm², and the PCE was decreased to 5.68%. From the series resistances (Rs) and shunt resistances (Rsh) of devices which were extracted from illuminated J-V curves, we found that the incorporating SQ decreases Rs compared to the control device. It indicates the better contact between the active layer and electrodes in ternary devices. The Rsh of the device with 15wt% SQ-BP was

extremely low (373.34 Ω cm² compared to 535.27 Ω cm² for control device), which indicates a large leakage current across the cell and contributes to the lower FF. On the contrary, the Voc of the devices were not significantly affected by the additive of SQ-BP for that the difference between ternary devices and control devices are only 0.02V.

Fig. 2(c) shows the EQE of PCDTBT:PC₇₁BM:SQ-BP devices with different SQ-BP concentrations in the active layer. The



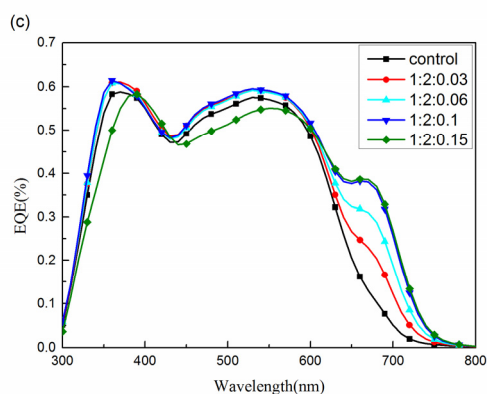


Fig.2 Solar Cell Performance. (a) The ultraviolet–visible (UV–Vis) absorption spectra of the PCDTBT neat film, SQ-BP neat film and PCDTBT:PC₇₁BM:SQ-BP (1:2:x) ternary blend films. (b) The current density – voltage (J–V) characteristics of PCDTBT:PC₇₁BM:SQ-BP (1:2:x) devices with different SQ-BP concentrations in the active layer under AM 1.5 G illumination with an intensity of 100 mW/cm². (c) The EQE of PCDTBT:PC₇₁BM:SQ-BP devices with different SQ-BP concentrations in the active layer.

enhancements in EQE can be divided into two parts, 350nm-600nm and 600nm-800nm. The EQE of ternary devices with SQ-BP concentration less than 15wt% in 350nm-600nm increased compared to the control PCDTBT:PC₇₁BM device which can be attributed to the additional exciton dissociation and charge carriers collection induced by the introduction of SQ-BP. The absorption of SQ-BP strongly overlaps with the photoluminescence of PCDTBT as shown in Fig. 1(d). We suppose that FRET is responsible for the increase of EQE in this range. In a neat PCDTBT film, a part of the photo-excited PCDTBT may turn back to ground state through recombination and does not result in photocurrent. When nearby SQ-BP molecules are present, some of photo-excited PCDTBT non-radiatively transfers energy to SQ-BP, which eventually improve the utilization of the energy of incident photons in the range of 350-600nm. Tenghooi Goh et al. have also reported a similar phenomenon.³⁸ But further adding SQ-BP to 15wt% led to lower

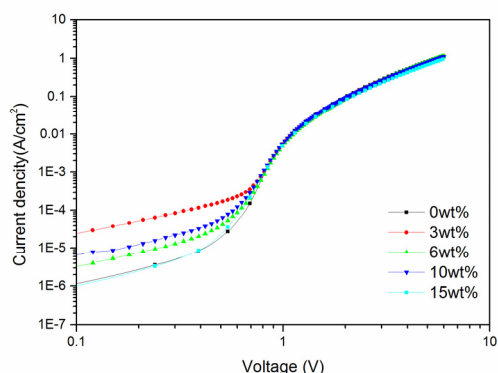


Fig.3 Dark J–V characteristics of ternary hole-only devices with different concentration of SQ-BP (0wt%, 3wt%, 6wt%, 10wt% and 15wt%) used for hole mobility measurement.

EQE in 300-600nm, which indicates that over doped SQ-BP disturbs the carrier transport in blend film. It can be further proved by the carrier mobility of blend films herein below. The EQE in 600-800nm monotonically increase strongly associate with the concentration of SQ-BP in the devices, which is a direct consequence of SQ-BP absorbing photons in this region.

The hole mobility of SQ-BP ($\sim 2.13 \times 10^{-5} \text{ cm}^2/\text{Vs}$) is lower than PCDTBT ($\sim 1.84 \times 10^{-4} \text{ cm}^2/\text{Vs}$). In order to learn whether the addition of SQ-BP did harms to the hole mobility of PCDTBT:PC₇₁BM film or not, hole-only devices were fabricated with the structures of ITO/MoO₃/ternary film/Au. We measured dark J–V characteristics of the devices and then fitted the results by using space charge-limited current (SCLC) model.³⁹⁻⁴¹ The current density is given by

$$J = \frac{9}{8} \epsilon_0 \epsilon_r \mu \frac{V^2}{L^3} \quad (1)$$

where ϵ_0 is the permittivity of free-space, ϵ_r is the relative dielectric constant of the active layer, L is the thickness of the active layer, and μ is the mobility. The dark J–V characteristics of the hole-only devices are shown in Fig.3. Through the equation (1), we can get the value of hole mobility. The hole mobility of blend films whose concentration of SQ-BP was 0wt%, 3wt%, 6wt%, 10wt% and 15wt% were $\sim 1.10 \times 10^{-4} \text{ cm}^2/\text{Vs}$, $\sim 1.06 \times 10^{-4} \text{ cm}^2/\text{Vs}$, $\sim 1.05 \times 10^{-4} \text{ cm}^2/\text{Vs}$, $\sim 1.03 \times 10^{-4} \text{ cm}^2/\text{Vs}$ and $\sim 8.55 \times 10^{-5} \text{ cm}^2/\text{Vs}$, respectively. It demonstrated that the addition of small amount of SQ-BP had little impact on the carrier transport of blend films. Therefore SQ-BP is a appropriate material for ternary solar cell base on PCDTBT:PC₇₁BM host film. It's worth noting that over doped SQ-BP can disturb the carrier transport in blend films, which would ultimately lead to lower J_{sc} and PCE of the devices.

The energy level diagram of devices is shown in Fig 1(c). The highest occupied molecular orbital (HOMO) of PCDTBT is between SQ-BP and PC₇₁BM. The LUMO of PCDTBT and SQ-BP are almost same and their energy level offset to PC₇₁BM is 0.7 eV. Such an energy gradient of PCDTBT:PC₇₁BM:SQ-BP matrix provides a feasibility of exciton dissociation and charge carriers transfer at both interfaces of PCDTBT/PC₇₁BM and SQ-BP/PC₇₁BM.^{42,43} When an incidence photon is absorbed by the active layer, a geminate exciton can be generated, which will eventually turn back to the ground state either by the non-radiative or radiative relaxation. These will lead to the energy loss of the device. But through FRET, the geminate recombination loss can be partially “recovered” by transferring energy to the FRET acceptor molecule for the exciton generation.³⁸ FRET is a non-radiative energy transfer process that acts through long-range dipole–dipole interactions between donor and acceptor molecules.³⁴ This process takes place with neither light emission of donor nor light absorption by the FRET acceptor, and leads to a reduction in the donor's fluorescence intensity and excited state lifetime. Incorporating SQ can provides another energy transfer route from excited PCDTBT molecules to SQ-BP molecules, which finally result in more excitation being harvested in the ternary films. Therefore, there may be three routes for exciton generating and dissociated into charge: I) PCDTBT molecules absorb incidence photons and produce excitons, then parts of excitons are dissociated at the interfaces of PCDTBT and PC₇₁BM; II) SQ-BP molecules absorb incidence photons and produce excitons, then these excitons are dissociated at the interfaces of SQ-BP and PC₇₁BM; III) Part excitons of PCDTBT transfer energy to SQ-BP

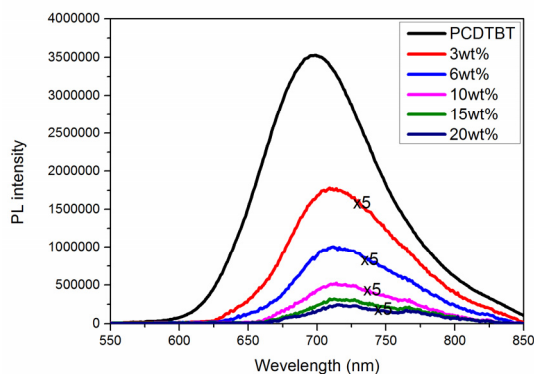


Fig. 4 Steady state photoluminescence (PL) spectra of neat PCDTBT film and SQ-BP:PCDTBT blend films with different SQ-BP concentration under the excitation of 373 nm light. All the intensity of SQ-BP:PCDTBT films are enlarged 5 times.

molecules to form excitons, then these excitons of SQ-BP formed by the energy transfer from PCDTBT are dissociated at the interfaces of SQ-BP and PC₇₁BM.

In order to further understand the possible dynamics processes of energy transfer and charge carriers transport in ternary devices, the photoluminescence (PL) of neat PCDTBT and blend PCDTBT:SQ-BP=1:x films were studied. The films for PL measurement were fabricated on optics quartz plates and the fabrication procedure was the same as that of devices fabrication. The PL spectra under the excitation of 373 nm are shown in Fig 4, in which the PL intensity of blend PCDTBT:SQ-BP=1:x films are enlarged 5 times. The PL emission peak of neat PCDTBT locates at 699 nm and the full width at half maximum is 96nm. The emission of PCDTBT was quenched severely with the additive of SQ-BP even when the concentration of SQ-BP was only 3wt%. The quenching efficiency (equation 2) can be used to quantify energy transfer from the relative peak intensity (I) in Fig 4. In this equation, I_{PCDTBT} is the PL intensity of PCDTBT at the emission peak of 699 nm, and I is the PL intensity of blend films at 714nm.

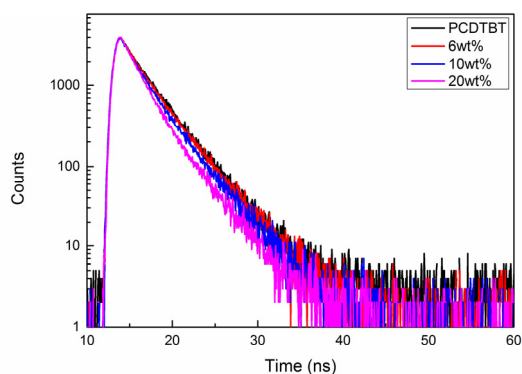


Fig. 5 The photoluminescence decay of neat PCDTBT and PCDTBT:SQ-BP=1:x ($x=6\text{wt}\%$, $10\text{wt}\%$ and $20\text{wt}\%$) films. The films were probed at 700nm under the excitation of 373nm pulse NanoLED source.

$$\phi_q = \frac{I_{PCDTBT} - I}{I_{PCDTBT}} \times 100\% \quad (2)$$

The values of ϕ_q for blend films with 3wt%, 6wt%, 10wt%, 15wt%, 20wt% SQ-BP were 89.93%, 94.40%, 97.02%, 98.23% and 98.64% respectively. Overall, the optical data strongly suggest that PCDTBT and SQ-BP are excellent candidates for forming an effective FRET pair in OPVs.

Photoluminescence decay measurements are aimed to assist in understanding the energy transfer between PCDTBT and SQ-BP. The neat PCDTBT, blend PCDTBT:SQ-BP=1:x ($x=6\text{wt}\%$, $10\text{wt}\%$, $20\text{wt}\%$) films were probed at 699nm under the excitation of 373nm pulse NanoLED source. The fluorescence decay of neat PCDTBT film and blended films, as shown in Fig. 5, were fitted with a two-component-exponential function. The lifetimes of 699 nm emission is about 2.91 ns for the neat PCDTBT film, $\sim 2.84\text{ns}$, $\sim 2.65\text{ns}$ and $\sim 2.31\text{ns}$ for 6wt%, 10wt% and 20wt% blend films respectively. The decrease of lifetime of excited state of PCDTBT indicates that the energy transfer process from PCDTBT to SQ-BP molecules has occurred. It is proved that the FRET from PCDTBT to SQ-BP molecule decreases the energy loss through radiative emission of excited PCDTBT molecules in ternary solar cell devices and provides a potential pattern for improving the photon utilization, which will eventually improve the performance of the photovoltaic devices.

Conclusions

In summary, we have successfully developed a novel BHJ ternary OPVs system with improved efficiency by incorporating SQ-BP into a PCDTBT:PC₇₁BM host blend. The PCE of PCDTBT:PC₇₁BM:SQ-BP ternary photovoltaic devices with 10wt% SQ-BP increased to 6.39% compared to 4.91% for PCDTBT:PC₇₁BM binary solar cells, which mainly due to the increasement of J_{sc} . The increasement of J_{sc} is caused both by the broader absorption spectrum of the ternary devices and an enhancement through FRET to decrease the energy loss of excited PCDTBT, which improves the photon utilization. Furthermore, we believe that there are still several methods can be used to optimize the already high efficiency of our devices, such as: (i) improving morphology of ternary film by annealing or solvent additives; (ii) choosing other charge injection layer to enhance the current collection. Overall, this study shows that the performance of OPVs can be increased by adopting ternary blend films, which has research significance on the industrialization of OPVs due to the effortless and low-cost fabrication process.

Acknowledgements

The project supported by "The Fundamental Research Funds for the Central Universities" No. S15JB00280 and "The Research Fund for the Doctoral Program of Higher Education" No. 20130009130001.

Notes and references

1. B. C. Thompson and J. M. Fréchet, *Angewandte Chemie International Edition*, 2008, **47**, 58-77.
2. G. Li, R. Zhu and Y. Yang, *Nature Photonics*, 2012, **6**, 153-161.
3. G. Nagarjuna and D. Venkataraman, *Journal of Polymer Science Part B: Polymer Physics*, 2012, **50**, 1045-1056.
4. N. Espinosa, M. Hösel, D. Angmo and F. C. Krebs, *Energy & Environmental Science*, 2012, **5**, 5117-5132.
5. Y. Liang, Z. Xu, J. Xia, S. T. Tsai, Y. Wu, G. Li, C. Ray and L. Yu, *Advanced Materials*, 2010, **22**, E135-E138.
6. Y. Liang and L. Yu, *Accounts of Chemical Research*, 2010, **43**, 1227-1236.
7. H. Sasabe, T. Igrashi, Y. Sasaki, G. Chen, Z. Hong and J. Kido, *RSC Advances*, 2014, **4**, 42804-42807.
8. D. Yang, Q. Yang, L. Yang, Q. Luo, Y. Chen, Y. Zhu, Y. Huang, Z. Lu and S. Zhao, *Chemical Communications*, 2014, **50**, 9346-9348.
9. P. Li, C. Sun, T. Jiu, G. Wang, J. Li, X. Li and J. Fang, *ACS Applied Materials & Interfaces*, 2014, **6**, 4074-4080.
10. X. Liu, H. Kim and L. J. Guo, *Organic Electronics*, 2013, **14**, 591-598.
11. V. Shrotriya, G. Li, Y. Yao, C.-W. Chu and Y. Yang, *Applied Physics Letters*, 2006, **88**, 073508.
12. Z. Li, H. C. Wong, Z. Huang, H. Zhong, C. H. Tan, W. C. Tsoi, J. S. Kim, J. R. Durrant and J. T. Cabral, *Nature Communications*, 2013, **4**, 2227.
13. B. Walker, A. B. Tamayo, X. D. Dang, P. Zalar, J. H. Seo, A. Garcia, M. Tantiwiwat and T. Q. Nguyen, *Advanced Functional Materials*, 2009, **19**, 3063-3069.
14. D. Huang, Y. Li, Z. Xu, S. L. Zhao, L. Zhao and J. Zhao, *Physical Chemistry Chemical Physics*, 2015, **17**, 8053-8060.
15. J. Y. Kim, K. Lee, N. E. Coates, D. Moses, T.-Q. Nguyen, M. Dante and A. J. Heeger, *Science*, 2007, **317**, 222-225.
16. B. E. Lassiter, J. D. Zimmerman, A. Panda, X. Xiao and S. R. Forrest, *Applied Physics Letters*, 2012, **101**, 063303.
17. C. C. Chen, W. H. Chang, K. Yoshimura, K. Ohya, J. B. You, J. Gao, Z. R. Hong and Y. Yang, *Advanced Materials*, 2014, **26**, 5670.
18. Z. He, C. Zhong, S. Su, M. Xu, H. Wu and Y. Cao, *Nature Photonics*, 2012, **6**, 591-595.
19. Y. H. Liu, J. B. Zhao, Z. K. Li, C. Mu, W. Ma, H. W. Hu, K. Jiang, H. R. Lin, H. Ade and H. Yan, *Nature Communications*, 2014, **5**.
20. L. Koster, V. Mihailetschi and P. Blom, *Applied Physics Letters*, 2006, **88**, 093511-093513.
21. V. S. Gevaerts, A. Furlan, M. M. Wienk, M. Turbiez and R. A. J. Janssen, *Advanced Materials*, 2012, **24**, 2130-2134.
22. B. E. Lassiter, J. D. Zimmerman, A. Panda, X. Xiao and S. R. Forrest, *Applied Physics Letters*, 2012, **101**.
23. B. E. Lassiter, J. D. Zimmerman and S. R. Forrest, *Applied Physics Letters*, 2013, **103**.
24. T. Ameri, P. Khoram, J. Min and C. J. Brabec, *Advanced Materials*, 2013, **25**, 4245-4266.
25. Y. J. Cho, J. Y. Lee, B. D. Chin and S. R. Forrest, *Organic Electronics*, 2013, **14**, 1081-1085.
26. B. A. Rao, M. S. Kumar, G. Sivakurnar, S. P. Singh, K. Bhanuprakash, V. J. Rao and G. D. Sharma, *ACS Sustainable Chemistry & Engineering*, 2014, **2**, 1743-1751.
27. M. Campoy-Quiles, Y. Kanai, A. El-Basaty, H. Sakai and H. Murata, *Organic Electronics*, 2009, **10**, 1120-1132.
28. Kokil, A. M. Poe, Y. Bae, A. M. Della Pelle, P. J. Homnick, P. M. Lahti, J. Kumar and S. Thayumanavan, *ACS Applied Materials & Interfaces*, 2014, **6**, 9920-9924.
29. X. Xiao, G. D. Wei, S. Y. Wang, J. D. Zimmerman, C. K. Renshaw, M. E. Thompson and S. R. Forrest, *Advanced Materials*, 2012, **24**, 1956-1960.
30. N. Li, F. Machui, D. Waller, M. Koppe and C. J. Brabec, *Solar Energy Materials and Solar Cells*, 2011, **95**, 3465-3471.
31. M. Koppe, H. J. Egelhaaf, G. Dennler, M. C. Scharber, C. J. Brabec, P. Schilinsky and C. N. Hoth, *Advanced Functional Materials*, 2010, **20**, 338-346.
32. L. Y. Lu, T. Xu, W. Chen, E. S. Landry and L. P. Yui, *Nature Photonics*, 2014, **8**, 716-722.
33. H. Mangold, A. A. Bakulin, I. A. Howard, C. Kastner, D. A. M. Egbe, H. Hoppe and F. Laquai, *Physical Chemistry Chemical Physics*, 2014, **16**, 20329-20337.
34. J. S. Huang, T. Goh, X. K. Li, M. Y. Sfeir, E. A. Bielinski, S. Tomasulo, M. L. Lee, N. Hazari and A. D. Taylor, *Nature Photonics*, 2013, **7**, 480-486.
35. J. M. Lobez, T. L. Andrew, V. Bulovic and T. M. Swager, *ACS Nano*, 2012, **6**, 3044-3056.
36. R. R. Lunt, T. P. Osedach, P. R. Brown, J. A. Rowehl and V. Bulovic, *Advanced Materials*, 2011, **23**, 5712-5727.
37. H. Sasabe, T. Igrashi, Y. Sasaki, G. Chen, Z. R. Hong and J. J. Kido, *RSC Advances*, 2014, **4**, 42804-42807.
38. T. Goh, J.-S. Huang, E. A. Bielinski, B. A. Thompson, S. Tomasulo, M. L. Lee, M. Y. Sfeir, N. Hazari and A. D. Taylor, *ACS Photonics*, 2014.
39. H. Azimi, A. Senes, M. C. Scharber, K. Hingerl and C. J. Brabec, *Advanced Energy Materials*, 2011, **1**, 1162-1168.
40. Z. C. He, C. M. Zhong, X. Huang, W. Y. Wong, H. B. Wu, L. W. Chen, S. J. Su and Y. Cao, *Advanced Materials*, 2011, **23**, 4636.
41. Q. Q. Yang, D. B. Yang, S. L. Zhao, Y. Huang, Z. Xu, X. D. Liu, W. Gong, X. Fan, Q. Y. Huang and X. R. Xu, *Applied Surface Science*, 2013, **284**, 849-854.
42. S. Karak, P. J. Homnick, A. M. Della Pelle, Y. Bae, V. V. Duzhko, F. Liu, T. P. Russell, P. M. Lahti and S. Thayumanavan, *ACS Applied Materials & Interfaces*, 2014, **6**, 11376-11384.
43. T. Ameri, J. Min, N. Li, F. Machui, D. Baran, M. Forster, K. J. Schottler, D. Dolfen, U. Scherf and C. J. Brabec, *Advanced Energy Materials*, 2012, **2**, 1198-1202.